

Received March 19, 2021, accepted April 2, 2021, date of publication April 12, 2021, date of current version April 21, 2021.

Digital Object Identifier 10.1109/ACCESS.2021.3072428

Decoupled Transmit and Receive Antenna Selection for Precoding-Aided Spatial Modulation

SANGCHOO KIM 

Department of Electronics Engineering, Dong-A University, Busan 604-714, South Korea

e-mail: sckim@dau.ac.kr

This work was supported by the Research Funds from Dong-A University.

ABSTRACT This paper proposes an optimal joint transmit and receive antenna subsets (TRASs) selection scheme for linear precoding-aided spatial modulation (PSM) systems. The optimal joint TRASs selection is performed by exhaustively searching, so that it is difficult to analyze an achievable diversity gain and it has a huge complexity. To tackle this problem, we propose a decoupled TRAS selection method which selects receive antenna subset (RAS) and transmit antenna subset (TAS) in a two-step serial manner. By computing a lower bound on the pairwise error probability and conducting extensive simulations, it is shown that the zero-forcing (ZF)-based PSM system with N_T transmit antennas, N_S selected transmit antennas, N_R receive antennas, and N_D selected receive antennas achieves diversity order of $(N_T - N_D + 1)(N_R - N_D + 1)$ even with TAS selection. Furthermore, decreasing the number of active transmit antennas by TAS selection after RAS selection is analytically shown to always degrade the bit error rate performance. The analysis results are validated by simulations. These analytical and simulation results can be regarded as natural extensions of earlier works on receive antenna selection and transmit antenna selection for the PSM systems. In addition, we study and compare two efficient algorithms for TRAS selection. First, incremental and decremental algorithms are employed for separable RAS and TAS successive selection, respectively, which have an excellent performance. It is analytically shown that the computational complexity of the first proposed decoupled suboptimal TRAS selection scheme is enormously reduced compared to the joint optimal and decoupled optimal algorithms. Second, an incremental TAS selection approach replaces the decremental strategy in the first TRAS selection algorithm to further reduce the complexity.


INDEX TERMS Joint transmit and receive antenna subset selection, transmit antenna selection, receive antenna selection, multiple input multiple output (MIMO), precoding, zero-forcing (ZF), spatial modulation (SM).

I. INTRODUCTION

In the recent years, the wireless communications community has witnessed diverse space-index modulation techniques proposed to obtain low-complexity and energy-efficient multiple-input multiple-output (MIMO) communication systems [1], [2]. Spatial modulation (SM) is an energy-efficient MIMO technique without inter-antenna interference since it enables single-stream decoding and obtains multiplexing gain with a single radio-frequency (RF) chain. By exploiting a new degree of freedom, i.e., spatial indexing at the transmitter, SM schemes convey spatial information bits in each

time slot [3]–[6]. Meanwhile, precoding-aided spatial modulation (PSM) can carry extra information bits by appropriately selecting a receive antenna index in the downlink MIMO systems [7]–[12]. In PSM, the transmit signals are precoded at the transmitter side to steer at a single receive antenna in each transmission and thus only a single RF chain can be equipped at the receiver side. Because of facilitating a simple receiver structure, the PSM scheme has attracted extensive research interests in the last few years.

To improve the transmission performance of space modulation schemes, various antenna subset selection techniques, which are capable of offering a high diversity, have been examined for the space modulation-based MIMO systems [13]–[22]. The system reliability in space modulation

The associate editor coordinating the review of this manuscript and approving it for publication was Filbert Juwono .

can be enhanced by using redundant transmit antennas and/or redundant receive antennas. Previous works on antenna subset selection cover either transmit antenna subset (TAS) selection or receive antenna subset (RAS) selection. TAS selection has been considered for the SM systems [13]–[16] and for the PSM systems [17]–[19]. RAS selection has been studied for the PSM systems [20]–[22]. In [18], the effects of only TAS selection on the bit error rate (BER) performance of the zero-forcing (ZF)-based PSM systems have been investigated. In [19], two TAS selection schemes with low-complexity have been developed for the PSM systems. In [20], optimal and greedy algorithms are considered to select an RAS for the PSM systems. In [21], two efficient RAS selection algorithms have been presented for the PSM systems. It is shown in [22] that the ZF-based PSM system performing only optimal RAS selection can achieve diversity order of $(N_T - N_D + 1)(N_R - N_D + 1)$ when N_T transmit antennas, N_R receive antennas, and N_D selected receive antennas are given.

A main drawback of massive MIMO systems is the high system complexity and hardware energy consumption. Employing a large number of antennas at the base station might be inexpensive. However, connecting an RF chain to each antenna element in massive MIMO is burdensome from an implementation standpoint [23], [24]. Therefore, antenna subset selection techniques have been actively investigated as one of solutions to alleviate the requirement on the number of RF transceivers. Even though various techniques with low RF-cost are recently being developed, the antenna subset selection method is still considered as a simple technique. Meanwhile, antenna subset selection has been incorporated into IEEE 802.11n standard [25] for performance improvement and range enhancement. Furthermore, it has been demonstrated in [26] that all antennas of the massive MIMO systems do not contribute equally in real propagation environments. When the traffic load is low, the power consumption is minimized by using only a subset of the available antennas [27]. From the practical viewpoint of implementation, the numbers of available RF chains both at the transmitter side and receiver side will be less than the numbers of transmit and receive antennas, respectively.

Thus, in a practical space modulation-based MIMO system, it is desirable to employ antenna subsets selection at both the transmitter and receiver sides. With joint transmit and receive antenna subsets (TRASs) selection, limited subsets of all available transmit and receive antennas can be used with reduced numbers of RF chains at both sides. Finding an optimal TRAS requires an exhaustive search, which is usually computationally prohibitive. Finding suboptimal algorithms for TRAS selection in conventional MIMO systems has been the subject of several efforts, which can be found in [28], [29]–[31], and [32]. In [28], [29], and [30], channel capacity is adopted as the performance metric for antenna selection. In [31], a joint TRAS selection problem for space-time coded systems is examined through a pairwise error probability (PEP) analysis. In [32], an enhanced joint transmitter-receiver spatial modulation scheme is proposed

by utilizing joint power allocation and antenna selection. But to the best of our knowledge, no study has been previously made for joint TRAS selection in the PSM-based MIMO systems.

In this paper, we consider the problem of joint TRAS selection in the PSM-based MIMO systems. First of all, an optimal joint TRAS selection algorithm is presented based on the criterion of maximizing the equivalent channel gain. As an initial step to reduce the complexity of the optimal joint TRAS selection algorithm based on an exhaustive two-dimensional search, a decoupled strategy is considered. We first select an RAS and then perform TAS selection using the pre-determined RAS. The decoupled TRAS selection scheme using separate optimal RAS and TAS selection makes us ease analytical tractability for the diversity gain that the ZF-based PSM system can provide when the decoupled approach is employed. Thus, we obtain the achievable diversity order through a PEP analysis. It is analytically shown that TAS selection after performing RAS selection does not degrade the diversity gain compared to that of the ZF-PSM systems without TAS selection. However, the array gain with TAS selection is analytically shown to be lower than that of the ZF-PSM systems without TAS selection.

Motivated to reduce the computational complexity, incremental and decremental strategies, respectively, are adopted for RAS selection and TAS selection. We first select an RAS by means of an incremental algorithm, and then TAS selection is decrementally performed on the subchannel resulting from RAS selection. Computational complexity analysis shows that the suboptimal decoupled TRAS selection method based on incremental RAS and decremental TAS selection offers tremendous complexity reduction compared with the optimal exhaustive search-based TRAS selection algorithm. In massive MIMO systems, the complexity of the decremental TAS selection algorithm is relatively high if the number of selected transmit antennas is much less than the total number of available transmit antennas. For further complexity reduction, TAS selection can be done via an incremental approach.

It should be pointed out that the decremental and incremental TAS algorithms proposed in [18] and [19] are employed for the second step (i.e., TAS selection) in the decoupled TRAS selection scheme of this work. Note that [18] and [19] consider only TAS selection. By contrast, this work proposes an optimal joint TRAS selection scheme for the PSM systems as we have said above. The optimal joint TRAS selection requires an exhaustive searching algorithm. To tackle the huge complexity, a decoupled TRAS selection method is proposed in a two-step serial manner. Moreover, the achievable diversity order of the PSM system with joint TRAS selection is analytically provided and also verified by simulation results.

The remainder of this paper is organized as follows. In Section II, the PSM system model with joint optimal TRAS selection is presented. In Section III, the decoupled TRAS selection algorithms for the ZF-PSM MIMO systems are considered together with the computational complexity

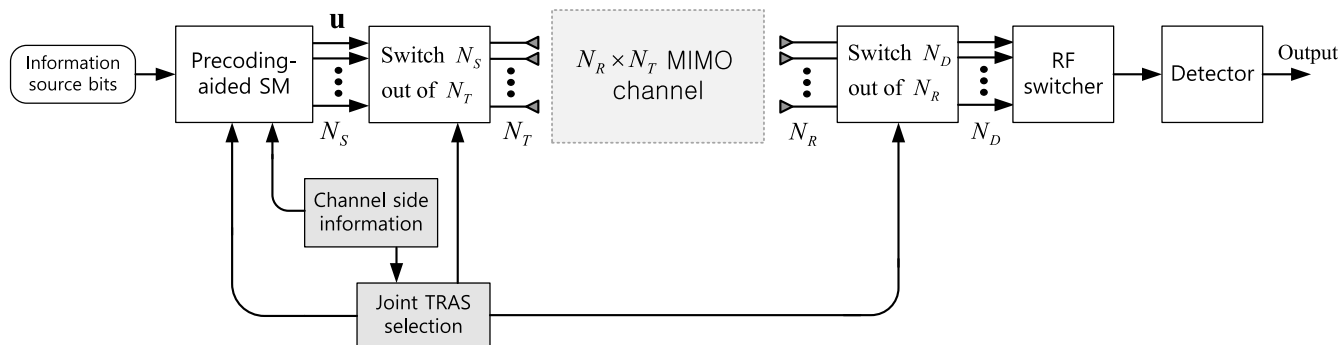


FIGURE 1. Block diagram of a PSM-MIMO TDD system with joint TRAS selection.

analysis. Section IV includes the diversity order analysis for the ZF-PSM MIMO systems with decoupled optimal TRAS selection. Simulation results are presented in Section V. Finally, some conclusions are drawn in Section VI.

Notation: Throughout this paper, boldface lower and upper case letters represent vectors and matrices, respectively. $(\cdot)^*$ and $(\cdot)^H$ denote the complex conjugate and the Hermitian transpose, respectively. $tr(\cdot)$ and $(\cdot)^{-1}$ stand for the trace operation and inverse operation, respectively. $E[\cdot]$, $\|\cdot\|$, and $\|\cdot\|_F$ denote the expectation, the Euclidean norm, and the Frobenius norm, respectively. \mathbf{I} and $Q(\cdot)$ are the identity matrix and the Q function, respectively.

II. PSM SYSTEM WITH JOINT TRAS SELECTION

Consider a PSM-MIMO time division duplex (TDD) system with N_T transmit antennas and N_R receive antennas as shown in Fig. 1. The transmitter and receiver, respectively, are equipped with $N_S (\leq N_T)$ RF transmission units and one RF receiving unit. It is assumed to have a block fading structure where each channel is static for a coherence period of channel uses. The full channel matrix is given as $\mathbf{H} \in C^{N_R \times N_T}$, whose elements are independent and identically distributed (i.i.d.) circularly symmetric complex Gaussian random variables with zero mean and unit variance. The perfect channel side information (CSI) of \mathbf{H} is assumed to be available at the transmitter and receiver.

In TDD mode, channel reciprocity between uplink and downlink channels can be exploited to estimate the CSI [33], [34]. The pilot symbols could be transmitted from each receive antenna through an uplink channel in a round-robin fashion among all the available receive antennas. The instantaneous CSI acquired at the transmitter can be utilized for precoding and joint TRAS selection. The indices of the selected RAS can be transmitted through a downlink channel or the RAS selection can be performed by exploiting the CSI estimated at the receiver side.

In this work, N_S antennas out of N_T transmit antennas and $N_D (\leq N_R)$ antennas out of N_R receive antennas are selected. To design the PSM system, it is required that $N_S \geq N_D$. The spatial modulated super-symbol vector is presented by $\mathbf{x} \in C^{N_D \times 1}$, which can be expressed as $\mathbf{x} = s_m \mathbf{e}_r$

where a symbol s_m with $E[s_m s_m^*] = 1$ is selected from the M -ary quadrature amplitude modulation (QAM) or phase-shift keying (PSK) constellation set and \mathbf{e}_r is the r -th column of the N_D -dimensional unit matrix. Since both m and r convey information, the data rate is given as $L = \log_2(M N_D)$ bit per channel use. The super-symbol \mathbf{x} is first precoded before transmission. Then the transmit signal vector $\mathbf{u} \in C^{N_S \times 1}$ is given by $\mathbf{u} = \mathbf{P} \mathbf{x}$ where $\mathbf{P} \in C^{N_S \times N_D}$ is a precoding matrix. The ZF and minimum mean square error precoding methods are commonly used in PSM. To be consistent with the previous works for the PSM systems [7], [8], [10], [11] and [18], we utilize the ZF precoding scheme in this paper. Then the ZF precoding matrix is given as

$$\mathbf{P}_{ZF} = \beta_U \mathbf{H}_U^H (\mathbf{H}_U \mathbf{H}_U^H)^{-1} \tag{1}$$

where $\mathbf{H}_U \in C^{N_D \times N_S}$ denotes the channel matrix obtained by joint TRAS selection and β_U is a power normalization factor used to ensure $E[\|\mathbf{u}\|^2] = 1$.

The received block signal at the receiver is described as

$$\mathbf{y} = \mathbf{H}_U \mathbf{P}_{ZF} \mathbf{x} + \mathbf{n} = \beta_U \mathbf{x} + \mathbf{n} \tag{2}$$

where the power normalization factor related with the selected TAS and RAS is

$$\beta_U = \sqrt{\frac{N_D}{tr[(\mathbf{H}_U \mathbf{H}_U^H)^{-1}]}} \tag{3}$$

and $\mathbf{n} \in C^{N_D \times 1}$ is an i.i.d. additive white Gaussian noise vector whose elements are the zero-mean circular complex white Gaussian noise component of a variance of σ_n^2 . Then the optimal joint TRAS selection algorithm (named as opt-TRAS) for the ZF-based PSM system can be expressed by

$$U^* = \underset{U \in \{U_k, k=1,2,\dots, C(N_T, N_S) \times C(N_R, N_D)\}}{\arg \max} \beta_U \tag{4}$$

where U_k is the k -th enumeration of the set of all available $C(N_T, N_S) \times C(N_R, N_D)$ antenna subsets. Here $C(N_T, N_S)$ and $C(N_R, N_D)$, respectively, are the total number of combinations of selecting N_S antennas among N_T transmit antennas and N_D antennas among N_R receive antennas. From the definition of the optimal β_U , the equation (4) can be rewritten

as

$$U^* = \underset{U \in \{U_k, k=1,2,\dots, C(N_T, N_S) \times C(N_R, N_D)\}}{\arg \min} \operatorname{tr} \left[(\mathbf{H}_U \mathbf{H}_U^H)^{-1} \right] \quad (5)$$

Note that the simulation results of the opt-TRAS in the Section V are obtained using (5).

In the receiver for ZF-based PSM, the optimal maximum likelihood (ML) detector is given by

$$\hat{\mathbf{x}} = \underset{\mathbf{x}}{\arg \min} \|\mathbf{y} - \beta U^* \mathbf{x}\|^2 \quad (6)$$

It is pointed out that the computational complexity of (5) to find an optimal TRAS is very high owing to an exhaustive search when the numbers of transmit antennas and receive antennas are large. To evaluate its computational complexity, we take account of the number of real multiplications (RMs) and the number of real summations (RSs) [18]–[21], [35]. The complexity of the exhaustive search-based optimal TRAS selection algorithm in terms of RMs and RSs, respectively, can be analyzed as

$$\begin{aligned} N_{opt-TRAS}^{RM} &= C(N_R, N_D)C(N_T, N_S) \\ &\quad \times (2N_S N_D^2 + 2N_S N_D + 2N_D^3 + 6N_D^2) \quad (7) \\ N_{opt-TRAS}^{RS} &= C(N_R, N_D)C(N_T, N_S) \\ &\quad \times (2N_S N_D^2 + 2N_S N_D + 2N_D^3 + N_D^2 + N_D) \quad (8) \end{aligned}$$

III. DECOUPLED TAS AND RAS SELECTION ALGORITHMS FOR ZF-PSM MIMO SYSTEMS

The optimal joint TRAS selection method for the ZF-PSM systems requires tremendous computational complexity. In this regard, a low-complexity TRAS selection algorithm needs to be developed. To reduce the overall complexity of the optimal joint TRAS selection scheme, the proposed suboptimal TRAS selection algorithm is based on decoupling RAS selection and TAS selection and thus consists of two consecutive antenna subsets selection steps. The proposed decoupled TRAS selection scheme is called a D-TRAS algorithm. As the first step, an RAS is selected. Then, TAS selection is carried out using the pre-selected RAS.

A. RAS SELECTION

Given N_T transmit antennas, the RAS selection problem to choose N_D antennas out of N_R receive antennas for the ZF-PSM systems can be expressed as

$$\begin{aligned} R^* &= \underset{R \in \{R_r, r=1,2,\dots, C(N_R, N_D)\}}{\arg \max} \sqrt{\frac{N_D}{\operatorname{tr} \left[(\mathbf{H}_R \mathbf{H}_R^H)^{-1} \right]}} \\ &= \underset{R \in \{R_r, r=1,2,\dots, C(N_R, N_D)\}}{\arg \min} \operatorname{tr} \left[(\mathbf{H}_R \mathbf{H}_R^H)^{-1} \right] \quad (9) \end{aligned}$$

where $\mathbf{H}_R \in C^{N_D \times N_T}$ is the channel matrix obtained by RAS selection. High computational complexity is required for this

TABLE 1. Suboptimal incremental RAS selection algorithm (D-inc-RAS).

Procedure	
Inputs: \mathbf{H}, N_D	
1:	$v(1) = \arg \max_{r \in \{1,2,\dots, N_R\}} \ \mathbf{h}_r\ ^2$
2:	$\mathbf{H}_R(1, :) = \mathbf{H}(v(1), :)$
3:	$\mathbf{\Pi}_1 = \mathbf{H}_R(1, :)\mathbf{H}_R^H(1, :)$
4:	$\mathbf{H}_Q = \mathbf{H}([1:(v(1)-1) \quad (v(1)+1): \text{end}], :)$
5:	for $i = 2 : N_D$
6:	for $j = 1 : (N_R - i + 1)$
7:	$\xi_{ij} = \mathbf{H}_R(1:(i-1), :)\mathbf{H}_Q^H(j, :)$
8:	$\mu_{ij} = \mathbf{H}_Q(j, :)\mathbf{H}_Q^H(j, :)$
9:	$\mathbf{\Pi}_i = [\mathbf{\Pi}_{i-1} \quad \xi_{ij} ; \xi_{ij}^H \quad \mu_{ij}]$
10:	$\alpha_j = \operatorname{tr}(\mathbf{\Pi}_i^{-1})$
11:	end
12:	$v(i) = \arg \min \{\alpha_1, \alpha_2, \dots, \alpha_{N_R-i+1}\}$
13:	$\mathbf{\Pi}_i = \mathbf{\Pi}_{v(i)}$
14:	$\mathbf{H}_R(i, :) = \mathbf{H}_Q(v(i), :)$
15:	$\mathbf{H}_Q = \mathbf{H}_Q([1:(v(i)-1) \quad (v(i)+1): \text{end}], :)$
16:	end
Output: \mathbf{H}_R	

exhaustive search-based RAS selection algorithm (called as D-opt-RAS). It is given as

$$\begin{aligned} N_{D-opt-RAS}^{RM} &= C(N_R, N_D)(2N_T N_D^2 + 2N_T N_D + 2N_D^3 + 6N_D^2) \quad (10) \\ N_{D-opt-RAS}^{RS} &= C(N_R, N_D) \\ &\quad \times (2N_T N_D^2 + 2N_T N_D + 2N_D^3 + N_D^2 + N_D) \quad (11) \end{aligned}$$

For RAS selection with substantially reduced complexity, an incremental antenna selection strategy is introduced. An RAS is constructed by adding receive antennas one by one in the incremental manner. Assuming that $(i-1)$ receive antennas are selected, the i -th receive antenna is selected according to the following criterion.

$$v(i) = \underset{j \in \{1,2,\dots, N_R-i+1\}}{\arg \min} \operatorname{tr} \left[(\mathbf{\Omega} \mathbf{\Omega}^H)^{-1} \right] \quad (12)$$

where $\mathbf{\Omega} = [\mathbf{H}_R(1:(i-1), :); \mathbf{H}_Q(j, :)] \in C^{i \times N_T}$. $\mathbf{H}_R(1:(i-1), :)$ corresponds to the channel submatrix selected during $(i-1)$ iterations and \mathbf{H}_Q is the channel matrix remained after removing the row vectors associated with the receive antennas selected up to the $(i-1)$ -th iteration. Thus, $\mathbf{H}_Q(j, :)$ is the j -th row vector of \mathbf{H}_Q formed after $(i-1)$ iterations. The proposed suboptimal incremental RAS selection algorithm is summarized in Table 1 and called as D-inc-RAS. Here the

first row vector is determined by maximizing the Euclidean norm as

$$v(1) = \arg \max_{r \in \{1, 2, \dots, N_R\}} \|\mathbf{h}_r\|^2 \quad (13)$$

where \mathbf{h}_r denotes the r -th row vector of the full channel matrix \mathbf{H} . In addition, (12) can be re-expressed as

$$v(i) = \arg \min_{j \in \{1, 2, \dots, N_R - i + 1\}} \text{Tr} \left(\begin{bmatrix} \mathbf{\Pi}_{i-1} & \boldsymbol{\xi}_{ij} \\ \boldsymbol{\xi}_{ij}^H & \mu_{ij} \end{bmatrix}^{-1} \right) \quad (14)$$

where

$$\mathbf{\Pi}_{i-1} = \mathbf{H}_R(1 : (i-1), :) \mathbf{H}_R^H(1 : (i-1), :) \quad (15)$$

$$\boldsymbol{\xi}_{ij} = \mathbf{H}_R(1 : (i-1), :) \mathbf{H}_Q^H(j, :) \quad (16)$$

$$\mu_{ij} = \mathbf{H}_Q(j, :) \mathbf{H}_Q^H(j, :) \quad (17)$$

The computational complexity of the D-inc-RAS selection algorithm in Table 1 is given by

$$\begin{aligned} N_{D\text{-inc-RAS}}^{RM} &= 4N_T N_R + 4N_T \\ &+ \sum_{i=2}^{N_D} (N_R - i + 1) (4N_T i + 2i^3 + 6i^2) \end{aligned} \quad (18)$$

$$\begin{aligned} N_{D\text{-inc-RAS}}^{RS} &= 4N_T N_R - 2N_R + 4N_T - 2 \\ &+ \sum_{i=2}^{N_D} (N_R - i + 1) \\ &\times \left((4N_T - 2)i + 2i^3 + 2i^2 + 2i \right) \end{aligned} \quad (19)$$

B. TAS SELECTION

After RAS selection, TAS selection can be performed in a way presented in [18]. Then, an upper bound on the average BER (ABER) for the PSM systems for a given $\mathbf{H}_S \in C^{N_D \times N_S}$, which is defined as the channel submatrix selected by the D-TRAS selection algorithm, is given as

$$\text{ABER} \leq \frac{1}{2^L} \sum_{p=1}^{2^L} \sum_{q=1}^{2^L} \frac{N(\mathbf{x}_p \rightarrow \mathbf{x}_q)}{L} E_{\mathbf{H}_S} \{ \text{PEP}_S(\mathbf{x}_p \rightarrow \mathbf{x}_q) \} \quad (20)$$

where L is the total number of bits conveyed in each transmission, $N(\mathbf{x}_p \rightarrow \mathbf{x}_q)$ is the number of bits in error between \mathbf{x}_p and \mathbf{x}_q , and $\text{PEP}_S(\mathbf{x}_p \rightarrow \mathbf{x}_q)$ denotes the PEP when \mathbf{x}_p is transmitted but \mathbf{x}_q is detected. From [18], the PEP for a given β_S is written as

$$\begin{aligned} \text{PEP}_S(\mathbf{x}_p \rightarrow \mathbf{x}_q) &= \Pr \left\{ \|\mathbf{y} - \beta_S \mathbf{x}_i\|^2 > \|\mathbf{y} - \beta_S \mathbf{x}_j\|^2 \right\} \\ &= Q \left(\sqrt{\left(\beta_S^2 / 2\sigma_n^2 \right) \|\mathbf{x}_p - \mathbf{x}_q\|^2} \right) \end{aligned} \quad (21)$$

where $\beta_S^2 = N_D / \text{tr} \left[(\mathbf{H}_S \mathbf{H}_S^H)^{-1} \right]$.

Then, minimizing the PEP of (21) is equivalent to maximizing the received signal-to-noise (rSNR) of $r\text{SNR}(S) = \beta_S^2 / \sigma_n^2$. Thus TAS selection after obtaining $\mathbf{H}_R \in C^{N_D \times N_T}$

by the RAS selection algorithm can be given as the following optimization.

$$\begin{aligned} S^* &= \arg \max_{S \in \{S_k, k=1, 2, \dots, C(N_T, N_S)\}} r\text{SNR}(S) \\ &= \arg \max_{S \in \{S_k, k=1, 2, \dots, C(N_T, N_S)\}} \frac{N_D}{\sigma_n^2 \text{tr} \left[(\mathbf{H}_S \mathbf{H}_S^H)^{-1} \right]} \end{aligned} \quad (22)$$

where S_k is the k -th enumeration of the set of all the available $C(N_T, N_S)$ TASs. By letting S be a TAS in the ZF-PSM systems, where $S \subset S' = \{1, 2, \dots, N_T\}$, it is shown in [18] and [37] that the optimal TAS that maximizes the $r\text{SNR}(S)$ corresponds to the TAS that minimizes the rSNR loss, which is defined in decibel as

$$r\text{SNR}_{dB}(\bar{S}) = 10 \log_{10} \left(1 + \frac{\text{tr}(\Phi_{\bar{S}})}{\text{tr}[\mathbf{\Xi}_{S'}]} \right) \quad (23)$$

where

$$\bar{S} = S' - S \quad (24)$$

$$\Phi_{\bar{S}} = \mathbf{\Xi}_{S'} \mathbf{H}_{\bar{S}} (\mathbf{I} - \mathbf{H}_{\bar{S}}^H \mathbf{\Xi}_{S'} \mathbf{H}_{\bar{S}})^{-1} \mathbf{H}_{\bar{S}}^H \mathbf{\Xi}_{S'} \quad (25)$$

$$\mathbf{\Xi}_{S'} = (\mathbf{H}_R \mathbf{H}_R^H)^{-1} \quad (26)$$

If $\text{tr}[\mathbf{\Xi}_{S'}]$ and N_D / σ_n^2 are fixed, the TAS selection problem for the ZF-PSM systems can be expressed as [18]

$$S_{opt} = \arg \min_{S \in \{S_k, k=1, 2, \dots, C(N_T, N_S)\}} \text{tr}(\Phi_{\bar{S}}) \quad (27)$$

The TAS selection algorithm of (27) is called as D-opt-TAS. Its complexity is analyzed as

$$\begin{aligned} N_{D\text{-opt-TAS}}^{RM} &= 2N_T N_D^2 + 2N_T N_D + 4N_D^3 + 8N_D^2 \\ &+ C(N_T, N_S) \times \left(2(N_T - N_S)^3 + (6N_D + 6)(N_T - N_S)^2 \right. \\ &\left. + (6N_D^2 + 4N_D)(N_T - N_S) \right) \end{aligned} \quad (28)$$

$$\begin{aligned} N_{D\text{-opt-TAS}}^{RS} &= 2N_T N_D^2 + 2N_T N_D + 4N_D^3 + 2N_D^2 - 2N_D \\ &+ C(N_T, N_S) \times \left(2(N_T - N_S)^3 + (6N_D + 1)(N_T - N_S)^2 \right. \\ &\left. + 6N_D^2(N_T - N_S) + N_D - N_D^2 \right) \end{aligned} \quad (29)$$

Because of huge complexity of the optimal TAS selection algorithm of (27), a decremental TAS selection algorithm considered in [18] is employed. It starts with the whole set of N_T transmit antennas using an $N_D \times N_T$ channel matrix \mathbf{H}_R and successively removes $(N_T - N_S)$ transmit antennas during $(N_T - N_S)$ iterations. At each iteration, one transmit antenna with the largest rSNR loss is removed. Then the decremental TAS selection algorithm is given in Table 2 and named as D-dec-TAS. For further complexity reduction, we adopt the incremental TAS selection algorithm given in Table 3, which is also introduced in [19], and called as D-inc-TAS. From

TABLE 2. Decremental TAS selection algorithm (D-dec-TAS) [18].

Procedure
Inputs: \mathbf{H}_R, N_T, N_S
1: $\mathbf{H}_t = \mathbf{H}_R$
2: compute $\Xi_t = (\mathbf{H}_t \mathbf{H}_t^H)^{-1}$
3: for $i = 1, 2, \dots, (N_T - N_S)$
4: $\mathbf{\Pi}_i = \Xi_t \Xi_t^H$
5: for $j = 1, 2, \dots, (N_T - i + 1)$
6: $\beta_j = \frac{\mathbf{H}_t^H(:, j) \mathbf{\Pi}_i \mathbf{H}_t(:, j)}{1 - \mathbf{H}_t^H(:, j) \Xi_t \mathbf{H}_t(:, j)}$
7: end
8: $\hat{j} = \arg \min \{\beta_1, \beta_2, \dots, \beta_{N_T-i+1}\}$
9: $\Xi_t = \Xi_t + \frac{\Xi_t \mathbf{H}_t(:, \hat{j}) \mathbf{H}_t^H(:, \hat{j}) \Xi_t}{1 - \mathbf{H}_t^H(:, \hat{j}) \Xi_t \mathbf{H}_t(:, \hat{j})}$
10: $\mathbf{H}_t = \mathbf{H}_t(:, [1: (\hat{j} - 1) (\hat{j} + 1): \text{end}])$
11: end
12: $\mathbf{H}_S = \mathbf{H}_t$
Output: \mathbf{H}_S

Table 2 and 3, their computational complexity in terms of RMs and RSs, respectively, can be evaluated as

$$\begin{aligned}
 N_{D\text{-dec-TAS}}^{RM} &= 2N_T N_D^2 + 2N_T N_D + 2N_D^3 + 6N_D^2 \\
 &+ \sum_{i=1}^{N_T-N_S} \left[2N_D^3 + 2N_D^2 + (N_T - i + 1)(8N_D^2 + 8N_D) \right]
 \end{aligned} \tag{30}$$

$$\begin{aligned}
 N_{D\text{-dec-TAS}}^{RS} &= 2N_T N_D^2 + 2N_T N_D + 3N_D^3 + 2N_D^2 - N_D \\
 &+ \sum_{i=1}^{N_T-N_S} \left[(N_T - i + 1)(8N_D^2 + 4N_D - 4) + N_D^3 + 2N_D^2 - N_D \right]
 \end{aligned} \tag{31}$$

$$\begin{aligned}
 N_{D\text{-inc-TAS}}^{RM} &= \sum_{n=1}^{N_S} (N_T + 1 - n)(6N_D^2 + 6N_D + 1)
 \end{aligned} \tag{32}$$

$$\begin{aligned}
 N_{D\text{-inc-TAS}}^{RS} &= \sum_{n=1}^{N_S} (N_T + 1 - n)(5N_D^2 + 5N_D - 1)
 \end{aligned} \tag{33}$$

Thus the overall complexities of the proposed optimal and two suboptimal D-TRAS selection algorithms, respectively, can be obtained as

$$N_{D\text{-opt-TRAS}}^{RM} = N_{D\text{-opt-RAS}}^{RM} + N_{D\text{-opt-TAS}}^{RM} \tag{34}$$

TABLE 3. Incremental TAS selection algorithm (D-inc-TAS) [19].

Procedure
Inputs: \mathbf{H}_R, N_T, N_S
1: $\bar{\mathbf{H}}_0 = \mathbf{H}_R$
2: $\Xi_0 = \mathbf{I}_{N_R}$
3: for $n = 1, 2, \dots, N_S$
4: for $q = 1, 2, \dots, (N_T - n + 1)$
5: $\Lambda_{n-1,q} = \frac{\Xi_{n-1}^H \bar{\mathbf{H}}_{n-1}(:, q) \bar{\mathbf{H}}_{n-1}^H(:, q) \Xi_{n-1}}{1 + \bar{\mathbf{H}}_{n-1}^H(:, q) \Xi_{n-1} \bar{\mathbf{H}}_{n-1}(:, q)}$
6: $\lambda_{n-1,q} = \text{tr} [\Xi_{n-1} - \Lambda_{n-1,q}]$
7: end
8: $\hat{q} = \arg \min_q \lambda_{n-1,q}$
9: $\mathbf{H}_S(:, n) = \bar{\mathbf{H}}_{n-1}(:, \hat{q})$
10: $\bar{\mathbf{H}}_n = \bar{\mathbf{H}}_{n-1}(:, [1: (\hat{q} - 1) (\hat{q} + 1): \text{end}])$
11: $\Xi_n = \Xi_{n-1} - \Lambda_{n-1,\hat{q}}$
12: end
Output: \mathbf{H}_S

$$N_{D\text{-opt-TRAS}}^{RS} = N_{D\text{-opt-RAS}}^{RS} + N_{D\text{-opt-TAS}}^{RS} \tag{35}$$

$$N_{\text{subopt-TRAS-A}}^{RM} = N_{D\text{-inc-RAS}}^{RM} + N_{D\text{-dec-TAS}}^{RM} \tag{36}$$

$$N_{\text{subopt-TRAS-A}}^{RS} = N_{D\text{-inc-RAS}}^{RS} + N_{D\text{-dec-TAS}}^{RS} \tag{37}$$

$$N_{\text{subopt-TRAS-B}}^{RM} = N_{D\text{-inc-RAS}}^{RM} + N_{D\text{-inc-TAS}}^{RM} \tag{38}$$

$$N_{\text{subopt-TRAS-B}}^{RS} = N_{D\text{-inc-RAS}}^{RS} + N_{D\text{-inc-TAS}}^{RS} \tag{39}$$

Here the first suboptimal D-TRAS selection algorithm (called subopt-TRAS-A) uses D-inc-RAS and D-dec-TAS while the second suboptimal D-TRAS selection approach (named subopt-TRAS-B) employs D-inc-RAS and D-inc-TAS. Further, it should be pointed out that the D-opt-TRAS selection algorithm performs D-opt-RAS selection and then D-opt-TAS selection.

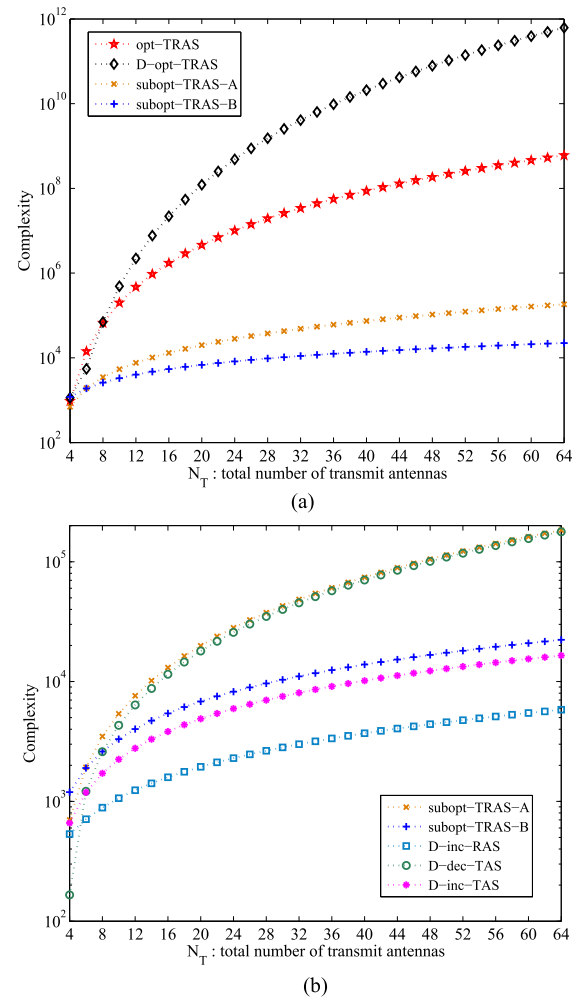
Table 4 shows that the two decoupled suboptimal TRAS selection algorithms can effectively reduce the complexity compared to the optimal TRAS and D-opt-TRAS selection algorithms. Particularly, for the large dimension of multiple antennas, the complexity of the two D-subopt-TRAS selection algorithms is tremendously lower than the optimal TRAS and D-opt-TRAS selection algorithms and the D-subopt-TRAS-B can achieve lower complexity than the D-subopt-TRAS-A.

Figs. 2(a), 3(a), and 4(a) compare the overall complexity (which is computed as a summation of RMs and RSs) of two the proposed D-subopt-TRAS selection algorithms with those of the optimal TRAS and D-opt-TRAS selection algorithms as a function of N_T for different combinations of N_S , N_R , and N_D . It is found that the proposed D-subopt-TRAS-A and D-subopt-TRAS-B selection algorithm can achieve significantly less complexity than the optimal TRAS and

TABLE 4. Computational complexity of RM and RS in different simulation scenarios.

SCENARIOS	TRAS ALGORITHM	RM	RS
$N_T = 3,$ $N_S = 2,$ $N_R = 3,$ $N_D = 2$	OPTIMAL TRAS	576	414
	D-OPT-TRAS	484	357
	D-SUBOPT-TRAS-A	420	324
	D-SUBOPT-TRAS-B	361	281
$N_T = 4,$ $N_S = 2,$ $N_R = 4,$ $N_D = 2$	OPTIMAL TRAS	2304	1656
	D-OPT-TRAS	1552	1188
	D-SUBOPT-TRAS-A	768	596
	D-SUBOPT-TRAS-B	555	441
$N_T = 8,$ $N_S = 4,$ $N_R = 4,$ $N_D = 2$	OPTIMAL TRAS	36960	29400
	D-OPT-TRAS	39056	30940
	D-SUBOPT-TRAS-A	1952	1532
	D-SUBOPT-TRAS-B	1434	1168
$N_T = 6,$ $N_S = 4,$ $N_R = 6,$ $N_D = 4$	OPTIMAL TRAS	86400	69300
	D-OPT-TRAS	12984	10780
	D-SUBOPT-TRAS-A	4832	4042
	D-SUBOPT-TRAS-B	4466	3640
$N_T = 8,$ $N_S = 4,$ $N_R = 8,$ $N_D = 4$	OPTIMAL TRAS	1881600	159200
	D-OPT-TRAS	112704	96360
	D-SUBOPT-TRAS-A	9344	7882
	D-SUBOPT-TRAS-B	7146	5908
$N_T = 16,$ $N_S = 4,$ $N_R = 4,$ $N_D = 2$	OPTIMAL TRAS	960960	764400
	D-OPT-TRAS	11707888	10218992
	D-SUBOPT-TRAS-A	7392	5692
	D-SUBOPT-TRAS-B	2970	2448
$N_T = 16,$ $N_S = 8,$ $N_R = 8,$ $N_D = 4$	OPTIMAL TRAS	490089600	421621200
	D-OPT-TRAS	49482304	43556680
	D-SUBOPT-TRAS-A	24096	20882
	D-SUBOPT-TRAS-B	18052	15186

D-opt-TRAS selection algorithms. Meanwhile, the complexity of the D-opt-TRAS selection algorithm is higher than that of the optimal TRAS one for large N_T . The reason is because opt-RAS selection and opt-TAS selection in the D-opt-TRAS selection algorithm require huge complexity for large N_T . Figs. 2(b), 3(b), and 4(b) compare the overall complexity

**FIGURE 2.** (a). Complexity comparison of suboptimal D-TRAS and optimal selection algorithms for $N_S = 4$, $N_R = 4$, and $N_D = 2$. (b). Complexity comparison of suboptimal RAS and TAS selection algorithms for $N_S = 4$, $N_R = 4$, and $N_D = 2$.

(which is RMs plus RSs) of the D-inc-RAS, D-dec-TAS, and D-inc-TAS selection algorithms used in the proposed D-subopt-TRAS-A and D-subopt-TRAS-B selection algorithms. It is seen that the complexity of the D-dec-TAS is higher than that of the D-inc-TAS for large N_T and thus is a dominant factor in that of the proposed D-subopt-TRAS-A.

IV. DIVERSITY ORDER FOR ZF-PSM MIMO SYSTEMS WITH D-OPT-TRAS SELECTION

It is well-known in [36] that when there exist N_T transmit antennas and N_R receive antennas, the transmit diversity order of the ZF-PSM MIMO systems without TAS and RAS selection is given as $N_T - N_R + 1$. Recently, it is shown in [22] that the ZF-PSM system selecting N_D receive antennas among N_R receive antennas, but without TAS selection can achieve diversity order of $(N_T - N_D + 1)(N_R - N_D + 1)$. Now, the achievable diversity order of the ZF-PSM system performing the D-opt-TRAS selection algorithm proposed in Section III is obtained by combining the analysis approaches presented in [18] and [22].

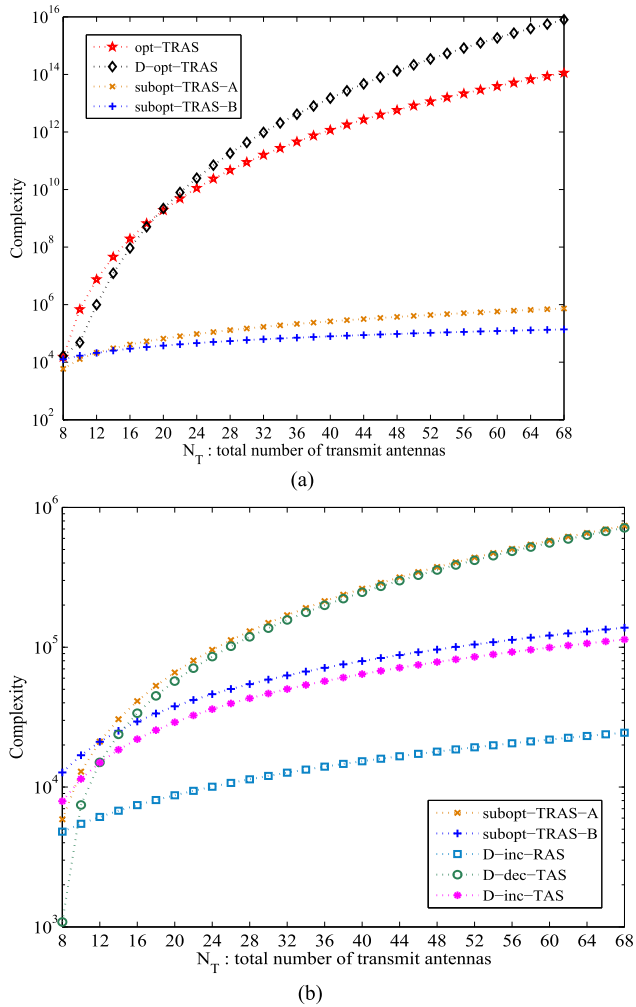


FIGURE 3. (a). Complexity comparison of suboptimal D-TRAS and optimal selection algorithms for $N_S = 8$, $N_R = 6$, and $N_D = 4$. (b). Complexity comparison of suboptimal RAS and TAS selection algorithms for $N_S = 8$, $N_R = 6$, and $N_D = 4$.

It is assumed that RAS selection is performed. After RAS selection, TAS selection is consecutively carried out under the determined RAS. Using Lemmas presented in [37], β_S^2 can be represented as

$$\beta_S^2 = \frac{N_D}{tr[\Xi_{S'}] + tr(\Phi_{\bar{S}})} \quad (40)$$

Since $tr(\Phi_{\bar{S}})$ is positive [37], we have

$$\beta_S^2 = L_S \beta_{S'}^2 \quad (41)$$

where L_S is the ratio of the rSNR between S and S' defined as

$$L_S = \frac{rSNR(S)}{rSNR(S')} = \frac{tr[\Xi_{S'}]}{tr[\Xi_{S'}] + tr(\Phi_{\bar{S}})} \quad (42)$$

Then the PEP of (21) can be rewritten as

$$PEP_S(\mathbf{x}_p \rightarrow \mathbf{x}_q) = Q \left(\sqrt{\frac{L_S \beta_{S'}^2}{2\sigma_n^2} \|\mathbf{x}_p - \mathbf{x}_q\|^2} \right) \quad (43)$$

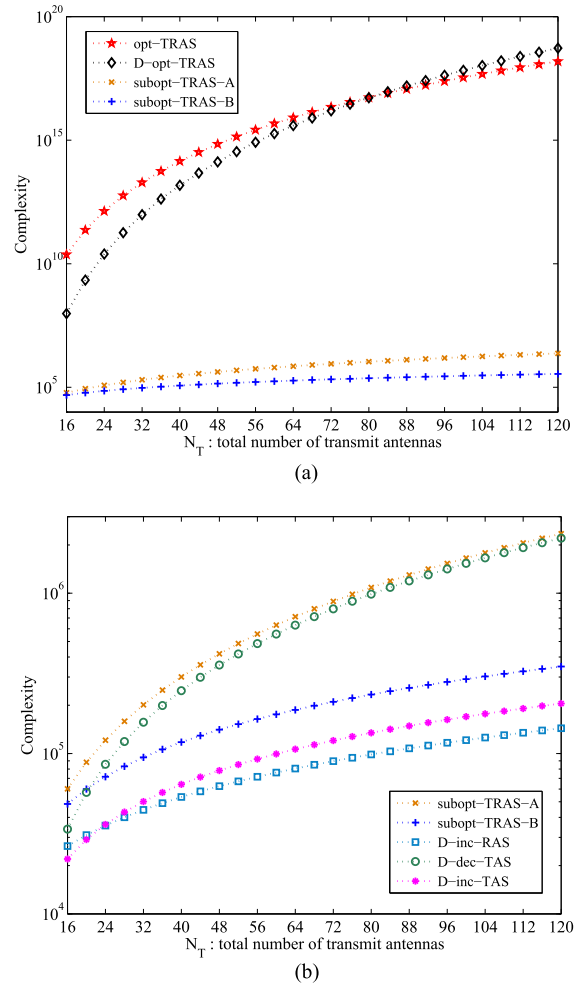


FIGURE 4. (a). Complexity comparison of suboptimal D-TRAS and optimal selection algorithms for $N_S = 8$, $N_R = 16$, and $N_D = 4$. (b). Complexity comparison of suboptimal RAS and TAS selection algorithms for $N_S = 8$, $N_R = 16$, and $N_D = 4$.

Assuming that the optimal RAS for a given channel realization \mathbf{H} is denoted by R_{k^0} , the PEP of (43) satisfies

$$PEP_{S'}(\mathbf{x}_p(k^0) \rightarrow \mathbf{x}_q(k^0)) \leq PEP_S(\mathbf{x}_p(k^0) \rightarrow \mathbf{x}_q(k^0)) \quad (44)$$

where \mathbf{x}_p and \mathbf{x}_q are any two distinct transmit signal vectors indexed by p and q in the optimal code book V_{k^0} and the lower bound of the PEP is defined as

$$PEP_{S'}(\mathbf{x}_p(k^0) \rightarrow \mathbf{x}_q(k^0)) = Q \left(\sqrt{\frac{\|\beta_{S'}(\mathbf{x}_p(k^0) - \mathbf{x}_q(k^0))\|_F^2}{2\sigma_n^2}} \right) \quad (45)$$

It is shown in [18] that the rSNR loss L_S is an array gain which can be served as a constant for a specific simulation setup. If N_S is not relatively small, especially for the ZF-PSM system with large N_T , the value of L_S generated by deleting only one antenna at each iteration might be small. Thus, $PEP_{S'}(\mathbf{x}_p(k^0) \rightarrow \mathbf{x}_q(k^0))$ can be employed as an approximated tight bound of $PEP_S(\mathbf{x}_p(k^0) \rightarrow \mathbf{x}_q(k^0))$ to derive the diversity order in this work. Then by using the

diversity analysis method used in [22], the ZF-PSM system based on D-TRAS selection can achieve diversity order of $(N_T - N_D + 1)(N_R - N_D + 1)$. It is noted that the product gain of $(N_T - N_D + 1)$ is supported by ZF precoding and another of $(N_R - N_D + 1)$ is achieved by RAS selection. Therefore, although both RAS selection and TAS selection are performed in the decoupled manner, the achievable diversity order of the ZF-PSM system with TRAS selection is the same as that of the ZF-PSM system with only RAS selection, but no TAS selection. The only difference is that TAS selection experiences the array gain loss of (42) while preserving the slope of BER.

V. SIMULATION RESULTS

This section shows through Monte Carlo simulations how the BER performance of the ZF-PSM systems varies owing to TRAS selection over Rayleigh flat-fading channels. For the performance comparison, the ZF-based PSM systems with subopt-TRAS-A selection, which is represented as D-subopt-TRAS in this section, are compared to those with opt-TRAS of (5) and D-opt-TRAS, which can be evaluated as benchmarks. The SNR is defined by the symbol energy to the noise power spectral density ratio, i.e., $\eta = 1/\sigma_n^2$. The QPSK modulation is assumed. The performance gain obtained by TRAS selection is compared with those of only RAS selection of [22] as well as only TAS selection of [18] and [19].

In the plots, $((N_T, N_S), (N_R, N_D))$ represents using N_T transmit antennas, N_S selected transmit antennas, N_R receive antennas, and N_D selected receive antennas as the system parameters for TRAS selection. $(N_S, (N_R, N_D))$ also represents using N_S transmit antennas without TAS selection, N_R receive antennas, and N_D selected receive antennas as the system parameters for only RAS selection. In addition, $((N_T, N_S), N_R)$ denotes using N_T transmit antennas, N_S selected transmit antennas, and N_R receive antennas with no RAS selection. Note that $((N_T, N_S), N_R)$ corresponds to the case with only TAS selection described in [18] and [19]. On the other hand, (N_S, N_D) symbolizes neither TAS selection or RAS selection (named no-TRAS). It has been shown in [18] that the numerical results of no-TAS selection for (N_S, N_D) are equivalent to those of random TAS selection for $((N_T, N_S), N_R)$ and thus the random TAS selection scheme has no selection diversity. It should be pointed out that even if the simulation results of decoupled random RAS selection and random TAS selection for joint TRAS selection of $((N_T, N_S), (N_R, N_D))$ are not given in this work, it may be anticipated that they would be exactly matched with those of no-TRAS selection for (N_S, N_D) . Furthermore, the BER reference curves are added into the same plots as a form of c/SNR^G with solid lines, where c is an appropriately selected positive constant and G denotes a diversity order, which determines a slope of BER curve.

Fig. 5 shows the BER performance of the ZF-PSM system for $N_S = 2$ and $N_D = 2$ with opt-TRAS selection. For performance comparison, the BER results of the ZF-PSM

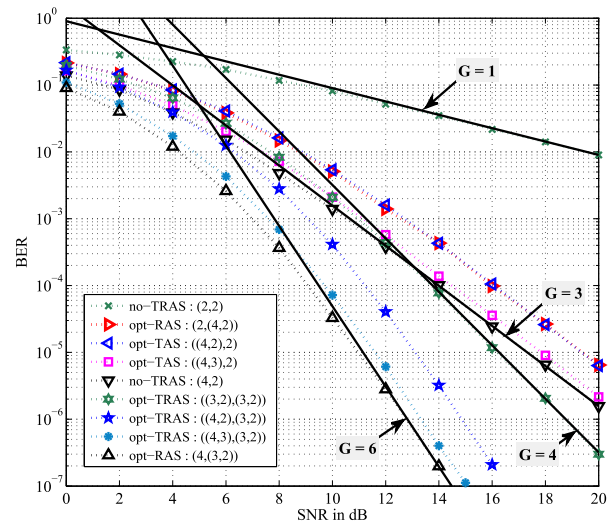


FIGURE 5. BER of optimal TRAS selection algorithm for ZF-PSM system with $N_S = 2$ and $N_D = 2$.

system with only optimal RAS selection [22] (called opt-RAS) and only optimal TAS selection [18] (called opt-TAS) are also included. Note that opt-RAS and opt-TAS, respectively, do not perform TAS selection and RAS selection. The former provides receive diversity and the latter does transmit diversity whereas the opt-TRAS selection approach can offer both receive and transmit diversity. It is thus shown that the opt-TRAS selection scheme for the $((3, 2), (3, 2))$ MIMO system with the diversity order of $G = 4$ outperforms the opt-RAS selection method for the $(2, (4, 2))$ MIMO system and the opt-TAS for the $((4, 2), 2)$ case, both of which present the same BER results with the diversity gain of $G = 3$. The $((4, 2), (3, 2))$ MIMO system can achieve much better performance than the $((3, 2), (3, 2))$ MIMO system because it has the diversity order of 6. Meanwhile, the $(4, (3, 2))$ ZF-PSM MIMO system with 4 active transmit antennas and opt-RAS selection can achieve the diversity order of 6. To plot the BER reference curves, the constants selected for $G = 1, 3, 4,$ and 6 , are $c = 0.9, 1.57, 32,$ and 49 , respectively. The $((4, 3), (3, 2))$ MIMO system with 3 active transmit antennas experiences the performance loss of about 0.6 dB while keeping the same diversity gain as the $(4, (3, 2))$ MIMO system. Obviously, the optimal RAS selection scheme offers the best performance owing to utilizing more RF chains. It should also be pointed out that TAS selection aims at reducing the number of RF chains and saves the power consumption at the transmitter. Although the diversity order has been derived for the D-opt-TRAS scheme, it is well-matched with the simulation results of the opt-TRAS. In addition, the $((4, 2), (3, 2))$ MIMO system with 2 active transmit antennas has the received SNR loss of about 2.1 dB compared to the $((4, 3), (3, 2))$ case. It is also found that they are well-matched with the analytical results in Fig. 10 plotted for the $rSNR_{dB}(\bar{S})$ of (23), which indicates the received SNR loss for the ZF-PSM system employing TAS selection. Thus, decreasing the number of active transmit

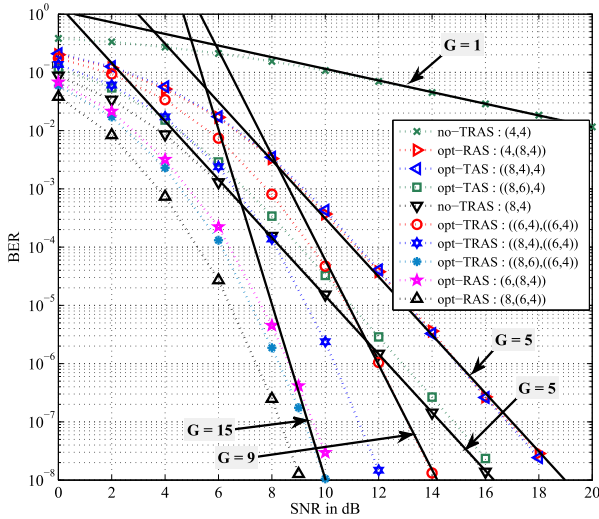


FIGURE 6. BER of optimal TRAS selection algorithm for ZF-PSM system with $N_S = 4$ and $N_D = 4$.

antennas for the ZF-PSM MIMO system with TRAS selection always degrades the BER performance.

In Fig. 6, the BER performances of the ZF-PSM system for $N_S = 4$ and $N_D = 4$ with opt-TRAS selection are presented. It is observed that the $((6, 4), (6, 4))$ MIMO system with opt-TRAS selection gives sufficiently higher performance than the $(4, (8, 4))$ MIMO system with opt-RAS selection and the $((8, 4), 4)$ case with opt-TAS selection. The former achieves the diversity order of $G = 9$ whereas the latter gives $G = 5$. It is also shown that the $(8, (6, 4))$ MIMO system with $G = 15$ can achieve significantly better performance than the $(8, 4)$ MIMO system with $G = 5$. The former can provide both transmit and receive diversity whereas the latter has only transmit diversity owing to ZF precoding. However, both the MIMO schemes require 8 RF transmission units at the transmitter. TAS selection can be employed to reduce the number of RF units at the transmitter side. Thus the $((8, 6), (6, 4))$ MIMO system with 6 active transmit antennas and 4 active receive antennas is capable of performing TAS and RAS selection. It has the diversity order of $G = 15$, which is the same as the $(8, (6, 4))$ case. But the array gain of the $((8, 6), (6, 4))$ MIMO system is about 1 dB less than the $(8, (6, 4))$ case and about 0.5 dB higher than the $(6, (8, 4))$ case. It is evident that the ZF-PSM system with TRAS selection results in better BER performance although the same number of RF chains is employed. The $((8, 4), (6, 4))$ MIMO system has the received SNR loss of about 3 dB compared with the $(8, (6, 4))$ case. They are well-matched with those of Fig. 10. Note that the constants employed for $G = 1, 5, 9,$ and $15,$ are $c = 1.15, 1.45(31), 6 \times 10^4,$ and $1.05 \times 10^7,$ respectively.

Figs. 7 and 8 give the BER performance comparison between the optimal TRAS and decoupled TRAS selection algorithms for the ZF-PSM MIMO systems. It is seen that the BER performance degradation of the D-opt-TRAS

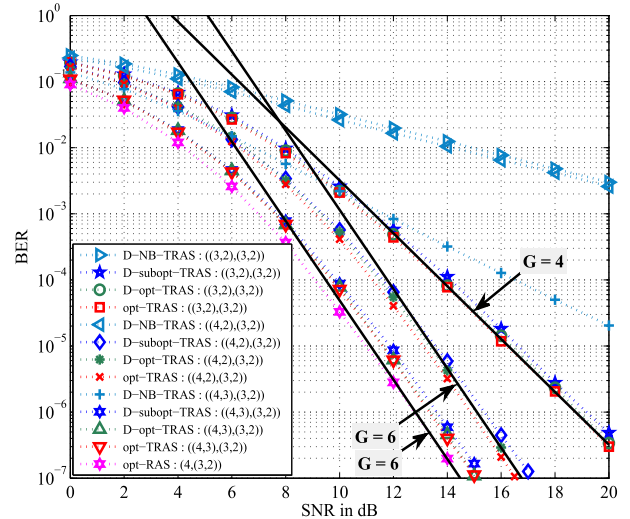


FIGURE 7. BER of optimal and decoupled TRAS selection algorithms for ZF-PSM system with $N_S = 2$ and $N_D = 2$.

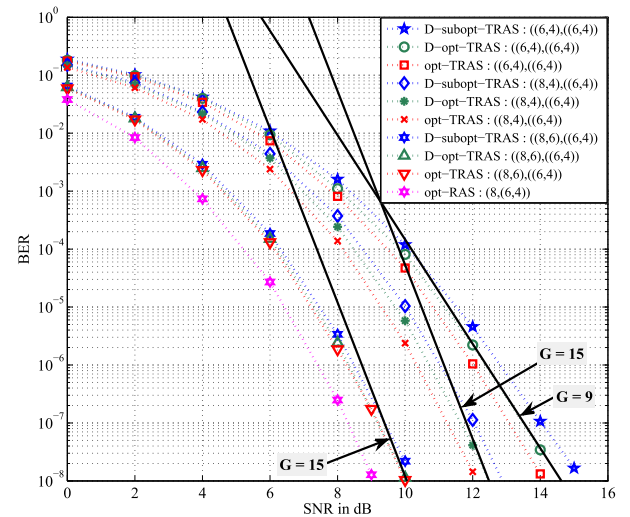


FIGURE 8. BER of optimal and decoupled TRAS selection algorithms for ZF-PSM system with $N_S = 4$ and $N_D = 4$.

selection scheme appears to be relatively small compared to the opt-TRAS. The proposed D-subopt-TRAS selection algorithm of subopt-TRAS-A with low-complexity shows slightly worse BER performance than the D-opt-TRAS. The $((4, 2), (3, 2))$ and $((8, 4), (6, 4))$ MIMO systems, respectively, outperform the $((3, 2), (3, 2))$ and $((6, 4), (6, 4))$ cases with identical TRAS selection because of having more transmit diversity gains. On the other hand, the $((4, 3), (3, 2))$ and $((8, 6), (6, 4))$ MIMO systems, respectively, have larger transmit antenna array gains compared to the $((4, 2), (3, 2))$ and $((8, 4), (6, 4))$ cases. However, note that the former two systems require 3 and 6 RF units at the transmitter whereas the latter two cases need 2 and 4 RF chains. For an additional comparison purpose, a simple decoupled norm-based TRAS (D-NB-TRAS) algorithm is simulated as a reference. It performs norm-based RAS selection and TAS selection in a

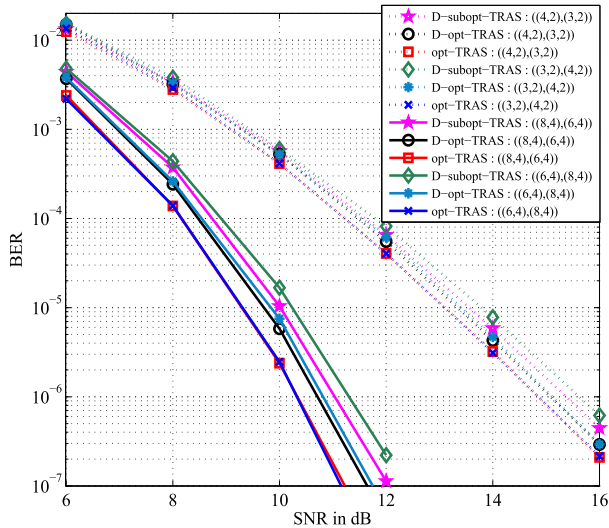


FIGURE 9. BER of optimal and decoupled TRAS selection algorithms for ZF-PSM system with the same diversity.

decoupling manner. The first RAS selection step selects N_D antennas out of N_R receive antennas that correspond to the N_D rows, which have the largest Frobenius norm among N_R rows of the full channel matrix \mathbf{H} . That is, the channel matrix $\mathbf{H}_R \in C^{N_D \times N_T}$ is obtained by RAS selection. Then the second TAS selection based on the norm values [18], [38] is conducted to get the channel matrix $\mathbf{H}_S \in C^{N_D \times N_S}$. It picks N_S antennas from N_T transmit antennas that is relevant to the N_S columns, which carry the largest norm out of N_T columns of the channel matrix \mathbf{H}_R . Its simulation results are presented in Fig. 7. It is observed that the proposed D-subopt-TRAS outperforms the D-NB-TRAS. Note that the constants used for $G = 4, 6, 9$, and 15 , are $c = 32, 49 (1150), 1.46 \times 10^5$, and $1.2 \times 10^7 (5.3 \times 10^{10})$, respectively.

In Fig. 9, the BER performances of the $((4, 2), (3, 2))$ and $((8, 4), (6, 4))$ MIMO systems using three TRAS selection algorithms are compared with those of the $((3, 2), (4, 2))$ and $((6, 4), (8, 4))$ system, respectively. Both the $((4, 2), (3, 2))$ and $((3, 2), (4, 2))$ systems have the same diversity order of 6. It is shown that the opt-TRAS and D-opt-TRAS selection algorithms, respectively, can achieve the similar performance for two systems. On the other hand, when the subopt-TRAS-A selection algorithm is used, the $((3, 2), (4, 2))$ system shows slightly worse performance than the $((4, 2), (3, 2))$ system. The reason is because suboptimal RAS selection followed by suboptimal TAS selection in the D-subopt-TRAS selection scheme is carried out from different numbers of the available receive and transmit antennas. Furthermore, the similar observations can be seen in the $((8, 4), (6, 4))$ and $((6, 4), (8, 4))$ systems.

Fig. 10 represents the analytical received SNR loss, $rSNR_{dB}(\bar{S})$, as a function of the number of selected transmit antennas for four different MIMO setup scenarios. It is shown that the value of $rSNR_{dB}(\bar{S})$ increases as the number of selected transmit antennas decreases. Note that the diversity order of $(N_T - N_D + 1)(N_R - N_D + 1)$, which is

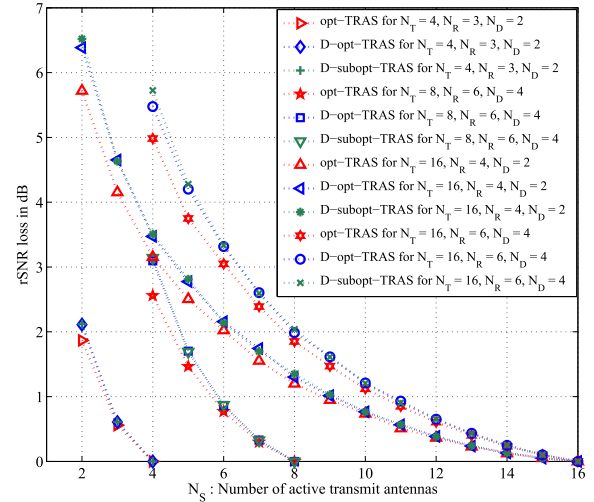


FIGURE 10. Received SNR loss for ZF-PSM system.

not a function of N_S , keeps the same even for the different numbers of selected transmit antennas. It is also found that the difference of the received SNR losses between opt-TRAS and D-TRAS gets slowly bigger as the number of selected transmit antennas decreases. This phenomenon can be similarly observed in the simulation results of Figs. 7, 8, and 9. By applying the analytical results to the massive MIMO cases with TRAS selection, the received SNR loss by TAS selection can be obtained even without the BER simulations requiring an excessive processing time.

VI. CONCLUSION

This paper presents a computational efficient joint transmit and receive antenna subsets (TRASs) selection scheme for the ZF-PSM MIMO systems. The proposed efficient TRAS selection approach is based on decoupling of transmit antenna subset (TAS) and receive antenna subset (RAS) selection. Thus two separate efficient TAS and RAS selections can be performed in sequence, where an incremental RAS selection algorithm is applied before conducting an independent incremental (or decremental) TAS selection algorithm. The computational complexity of the proposed decoupled efficient TRAS selection algorithm is significantly lower than that of the optimal exhaustive search. Moreover, it is shown that the ZF-PSM system with decoupled TRAS selection can achieve the diversity order of $(N_T - N_D + 1)(N_R - N_D + 1)$ where N_T , N_R , and N_D denote the numbers of transmit antennas, receive antennas, and selected receive antennas, respectively. It is observed that the proposed decoupled efficient TRAS selection algorithm offers slightly worse BER performance than the optimal one. In addition, the received SNR loss experienced from TAS selection after RAS selection is analytically obtained and well-matched with simulation results.

REFERENCES

- [1] E. Basar, "Index modulation techniques for 5G wireless networks," *IEEE Commun. Mag.*, vol. 54, no. 7, pp. 168–175, Jul. 2016.
- [2] R. Y. Mesleh and A. Alhassani, *Space Modulation Techniques*, 1st ed. Hoboken, NJ, USA: Wiley, 2018.

- [3] R. Y. Mesleh, H. Haas, S. Sinanovic, C. W. Ahn, and S. Yun, "Spatial modulation," *IEEE Trans. Veh. Technol.*, vol. 57, no. 4, pp. 2228–2241, Jul. 2008.
- [4] J. Jeganathan, A. Ghayeb, and L. Szczecinski, "Spatial modulation: Optimal detection and performance analysis," *IEEE Commun. Lett.*, vol. 12, no. 8, pp. 545–547, Aug. 2008.
- [5] M. Di Renzo, H. Haas, A. Ghayeb, S. Sugiura, and L. Hanzo, "Spatial modulation for generalized MIMO: Challenges, opportunities, and implementation," *Proc. IEEE*, vol. 102, no. 1, pp. 56–103, Jan. 2014.
- [6] M. Wen, B. Zheng, K. J. Kim, M. Di Renzo, T. A. Tsiftsis, K.-C. Chen, and N. Al-Dhahir, "A survey on spatial modulation in emerging wireless systems: Research progresses and applications," *IEEE J. Sel. Areas Commun.*, vol. 37, no. 9, pp. 1949–1972, Sep. 2019.
- [7] L.-L. Yang, "Transmitter preprocessing aided spatial modulation for multiple-input multiple-output systems," in *Proc. IEEE 73rd Veh. Technol. Conf. (VTC Spring)*, May 2011, pp. 1–5.
- [8] R. Zhang, L.-L. Yang, and L. Hanzo, "Generalised pre-coding aided spatial modulation," *IEEE Trans. Wireless Commun.*, vol. 12, no. 11, pp. 5434–5443, Nov. 2013.
- [9] J. Li, M. Wen, X. Cheng, Y. Yan, S. Song, and M. H. Lee, "Generalized precoding-aided quadrature spatial modulation," *IEEE Trans. Veh. Technol.*, vol. 66, no. 2, pp. 1881–1886, Feb. 2017.
- [10] P. Yang, Y. L. Guan, Y. Xiao, M. D. Renzo, S. Li, and L. Hanzo, "Transmit precoded spatial modulation: Maximizing the minimum Euclidean distance versus minimizing the bit error ratio," *IEEE Trans. Wireless Commun.*, vol. 15, no. 3, pp. 2054–2068, Mar. 2016.
- [11] O. Hiari and R. Mesleh, "Hardware design and analysis for generalized receive space modulation techniques," *IEEE Commun. Lett.*, vol. 23, no. 9, pp. 1616–1620, Sep. 2019.
- [12] C. Liu, L.-L. Yang, and W. Wang, "Transmitter-precoding-aided spatial modulation achieving both transmit and receive diversity," *IEEE Trans. Veh. Technol.*, vol. 67, no. 2, pp. 1375–1388, Feb. 2018.
- [13] R. Rajashekar, K. V. S. Hari, and L. Hanzo, "Antenna selection in spatial modulation systems," *IEEE Commun. Lett.*, vol. 17, no. 3, pp. 521–524, Mar. 2013.
- [14] N. Pillay and H. Xu, "Comments on 'antenna selection in spatial modulation systems,'" *IEEE Commun. Lett.*, vol. 17, no. 9, pp. 1681–1683, Sep. 2013.
- [15] R. Rajashekar, K. V. S. Hari, and L. Hanzo, "Quantifying the transmit diversity order of Euclidean distance based antenna selection in spatial modulation," *IEEE Signal Process. Lett.*, vol. 22, no. 9, pp. 1434–1437, Sep. 2015.
- [16] P. Yang, Y. Xiao, Y. L. Guan, Z. Liu, S. Li, and W. Xiang, "Adaptive SM-MIMO for mmWave communications with reduced RF chains," *IEEE J. Sel. Areas Commun.*, vol. 35, no. 7, pp. 1472–1485, Jul. 2017.
- [17] Y. Huang, M. Wen, B. Zheng, X. Cheng, L. Yang, and F. Ji, "Secure precoding aided spatial modulation via transmit antenna selection," *IEEE Trans. Veh. Technol.*, vol. 68, no. 9, pp. 8893–8905, Sep. 2019.
- [18] S. Kim, "Transmit antenna selection for precoding-aided spatial modulation," *IEEE Access*, vol. 8, pp. 40723–40731, 2020.
- [19] S. Kim, "Efficient transmit antenna selection for receive spatial modulation-based massive MIMO," *IEEE Access*, vol. 8, pp. 152034–152044, 2020.
- [20] J. Zheng, "Fast receive antenna subset selection for pre-coding aided spatial modulation," *IEEE Wireless Commun. Lett.*, vol. 4, no. 3, pp. 317–320, Jun. 2015.
- [21] P. Wen, X. He, Y. Xiao, P. Yang, R. Shi, and K. Deng, "Efficient receive antenna selection for pre-coding aided spatial modulation," *IEEE Commun. Lett.*, vol. 22, no. 2, pp. 416–419, Feb. 2018.
- [22] S. Kim, "Diversity order of precoding-aided spatial modulation using receive antenna selection," *Electron. Lett.*, vol. 56, no. 5, pp. 260–262, Mar. 2020.
- [23] E. Björnson, E. G. Larsson, and T. L. Marzetta, "Massive MIMO: Ten myths and one critical question," *IEEE Commun. Mag.*, vol. 54, no. 2, pp. 114–123, Feb. 2016.
- [24] S. Asaad, A. M. Rabieci, and R. R. Müller, "Massive MIMO antenna selection: Fundamental limits and applications," *IEEE Trans. Wireless Commun.*, vol. 17, no. 12, pp. 8502–8516, Dec. 2018.
- [25] *Enhancements for Higher Throughput*. IEEE Standard 802.11n-2009, Oct. 2009. [Online]. Available: <http://www.ieee802.org>
- [26] X. Gao, O. Edfors, F. Tufvesson, and E. G. Larsson, "Massive MIMO in real propagation environments: Do all antennas contribute equally?" *IEEE Trans. Commun.*, vol. 63, no. 11, pp. 3917–3928, Nov. 2015.
- [27] K. Senel, E. Björnson, and E. G. Larsson, "Joint transmit and circuit power minimization in massive MIMO with downlink SINR constraints: When to turn on massive MIMO?" *IEEE Trans. Wireless Commun.*, vol. 18, no. 3, pp. 1834–1846, Mar. 2019.
- [28] A. Gorokhov, M. Collados, D. Gore, and A. Paulraj, "Transmit/receive MIMO antenna subset selection," in *Proc. IEEE Int. Conf. Acoust., Speech, Signal Process.*, May 2004, pp. 13–16.
- [29] C.-E. Chen, "A computationally efficient near-optimal algorithm for capacity-maximization based joint transmit and receive antenna selection," *IEEE Commun. Lett.*, vol. 14, no. 5, pp. 402–404, May 2010.
- [30] J.-K. Lain, "Joint transmit/receive antenna selection for MIMO systems: A real-valued genetic approach," *IEEE Commun. Lett.*, vol. 15, no. 1, pp. 58–60, Jan. 2011.
- [31] T. Gucluoglu and T. M. Duman, "Performance analysis of transmit and receive antenna selection over flat fading channels," *IEEE Trans. Wireless Commun.*, vol. 7, no. 8, pp. 3056–3065, Aug. 2008.
- [32] J. Luo, S. Wang, and F. Wang, "Joint transmitter-receiver spatial modulation design via minimum Euclidean distance maximization," *IEEE J. Sel. Areas Commun.*, vol. 37, no. 9, pp. 1986–2000, Sep. 2019.
- [33] J. Jose, A. Ashikhmin, T. L. Marzetta, and S. Vishwanath, "Pilot contamination and precoding in multi-cell TDD systems," *IEEE Trans. Wireless Commun.*, vol. 10, no. 8, pp. 2640–2651, Aug. 2011.
- [34] E. Björnson, J. Hoydis, M. Kountouris, and M. Debbah, "Massive MIMO systems with non-ideal hardware: Energy efficiency, estimation, and capacity limits," *IEEE Trans. Inf. Theory*, vol. 60, no. 11, pp. 7112–7139, Nov. 2014.
- [35] R. Hunger, "Floating point operations in matrix-vector calculus (Version 1.3)," Technische Universität München, München, German, Tech. Rep., 2007. [Online]. Available: <https://mediatum.ub.tum.de/doc/625604/625604.pdf>
- [36] J. H. Winters, J. Salz, and R. D. Gitlin, "The impact of antenna diversity on the capacity of wireless communication systems," *IEEE Trans. Commun.*, vol. 42, nos. 2–4, pp. 1740–1751, Feb. 1994.
- [37] P.-H. Lin and S.-H. Tsai, "Performance analysis and algorithm designs for transmit antenna selection in linearly precoded multiuser MIMO systems," *IEEE Trans. Veh. Technol.*, vol. 61, no. 4, pp. 1698–1708, May 2012.
- [38] S. Kim, "Performance of decremental antenna selection algorithms for spatial multiplexing MIMO systems with linear receiver over correlated fading channels," *IET Commun.*, vol. 11, no. 6, pp. 855–863, Apr. 2017.



SANGCHOON KIM was born in Jeju, South Korea, in 1965. He received the B.S. degree from Yonsei University, Seoul, South Korea, in 1991, and the M.E. and Ph.D. degrees from the University of Florida, Gainesville, FL, USA, in 1995 and 1999, respectively, all in electrical and computer engineering. From 2000 to 2005, he was a Senior Research Engineer with LG Corporate Institute of Technology, Seoul, and a Chief Research Engineer with the LG Electronics, Anyang, South Korea, where he was working on a range of research projects in the field of wireless/mobile communications. Since 2005, he has been with Dong-A University, Busan, South Korea, where he is currently a Professor with the Department of Electronics Engineering. His research interests include wireless/mobile communications, signal processing, and antenna design.

• • •